Gene Expression Profiling of Human Epidermal Keratinocytes in Simulated Microgravity and Recovery Cultures

Jade Q. Clement*, Shareen M. Lacy, and Bobby L. Wilson

Department of Chemistry and NASA University Research Center for Biotechnology and Environmental Health, Texas Southern University, Houston, TX 77004, USA.

Simulated microgravity (SMG) bioreactors and DNA microarray technology are powerful tools to identify "space genes" that play key roles in cellular response to microgravity. We applied these biotechnology tools to investigate SMG and post-SMG recovery effects on human epidermal keratinocytes by exposing cells to SMG for 3, 4, 9, and 10 d using the high aspect ratio vessel bioreactor followed by recovery culturing for 15, 50, and 60 d in normal gravity. As a result, we identified 162 differentially expressed genes, 32 of which were "center genes" that were most consistently affected in the time course experiments. Eleven of the center genes were from the integrated stress response pathways and were coordinately down-regulated. Another seven of the center genes, which are all metallothionein MT-I and MT-II isoforms, were coordinately up-regulated. In addition, HLA-G, a key gene in cellular immune response suppression, was found to be significantly up-regulated during the recovery phase. Overall, more than 80% of the differentially expressed genes from the shorter exposures ($\leq$4 d) recovered in 15 d; for longer ($\geq$9 d) exposures, more than 50 d were needed to recover to the impact level of shorter exposures. The data indicated that shorter SMG exposure duration would lead to quicker and more complete recovery from the microgravity effect.

Key words: HEK001, HARV, DNA microarray, Northern blotting, expression profiling, microgravity

Introduction

Exposure to microgravity has been recognized as a major environmental factor of spaceflight. Some of the adverse effects resulting from spaceflight are a decline in cellular immune response (*1–3*), cardiovascular deconditioning (*4*), bone deterioration (*5*), and muscular atrophy (*6*). Elucidation of the molecular mechanisms underlying microgravity-induced health problems is critical for formulating effective countermeasures for spaceflight side-effects. Due to the cost effectiveness and the ability to separate microgravity effect from other complex factors of spaceflight, ground-based simulated microgravity (SMG) research has become popular and is widely practiced in space life sciences research.

Ground-based SMG conditions for mammalian cell and microorganism cultures are created through the use of high aspect ratio vessel (HARV) bioreactors (*7, 8*), which simulate microgravity by maintaining the cells in continuous free fall in liquid medium and are most commonly used in the United States (*9–12*). The HARV bioreactor does not allow the cells to receive a gravitational load in any fixed direction. Its constant rotation does not eliminate gravity, but it does allow the g-vector to be time-averaged to near zero (*13*). Ground-based SMG experiments using bioreactors such as HARV have become increasingly recognized as an effective approach in simulating certain aspects of microgravity, as it readily permits the more detailed experimentation towards the understanding of microgravity effects on genes and cellular activities during microgravity exposure.

Understanding gene and cellular activity changes in microgravity is essential for tackling the problems caused by microgravity exposure and for developing potential countermeasures. Studies at the cellular and molecular levels have been reported from both spaceflight and ground-based microgravity simulators such as HARV (*10, 14–17*). Microgravity has been found to influence major cellular events such as cell

***Corresponding author.**
E-mail: clement_jq@tsu.edu

proliferation, cell cycle, cell differentiation, and programmed cell death (*18–20*). Many cell types, ranging from bacteria to mammalian cells, are sensitive to the microgravity environment, suggesting that microgravity affects fundamental cellular activities. The study of microgravity effects on cellular activities can benefit enormously from genome-wide gene expression technologies.

Gene expression profiling based on DNA microarrays is a genome-wide gene expression analysis method for assessing cellular and molecular activity changes in response to a change in the growth environment. Environmental change as drastic as sudden gravity change is likely to alter the functions and transcriptional activities of groups of genes. A genome-wide display and comparison of gene expression profiles in cells that are exposed to microgravity and different recovery stages could provide great insight into the array of genes that are directly or indirectly involved in gravity response. This is because any change in the physiological activity of a cell is most likely the result of changes in the expression of certain genes. Thus, the genome-wide expression analysis technology can be a powerful tool to identify the "space genes" that play key roles in cellular response to a microgravity environment. In recent years, microarray technology has become increasingly popular in space biosciences research and most of the microgravity-induced cellular and molecular effects have been reported on cells of the immune system (*21*, *22*), muscle (*23–26*), and bone (*12, 27–30*). However, it is not clear if the affected cellular functions would recover once the cells are returned to 1 *g* conventional growth conditions.

To further understand the cellular and molecular mechanisms by which spaceflight alters cellular activities, the effects of microgravity on various human cell lines should be studied to identify the genes whose functions are most consistently affected by microgravity. Epidermal keratinocytes, the major cell type in the outermost layer of the skin, play an essential role in the first-line defense against invading microorganisms and in innate immunity (*31*, *32*). To date, the molecular effect of microgravity on keratinocytes is not known. Thus, the aim of this study was to display time course gene expression profiles and identify key gravity sensitive genes for human kerotinocytes in response to microgravity. We studied the microgravity effect on a basal-like type of immortalized human epidermal keratinocytes, HEK001, using the HARV bioreactor SMG system. We applied DNA microarray analysis for genome-wide expression profiling of the cells exposed to HARV bioreactor SMG conditions for 3, 4, 9, and 10 d, followed by recovery of 15, 50, and 60 d at 1 *g*. Our results indicated that cellular gene activity achieved >80% recovery from the shorter exposure time (≤4 d) in a recovery period of 15 d, while a longer recovery period (≥50 d) was needed for genes to recover to the shorter exposed impact levels after an exposure time as long as 9 and 10 d. In addition, we have identified 32 putative "major space genes" that were most consistently affected by SMG through the interlinked time course analysis. Interestingly, a cluster of eleven genes that are inducible through the integrated stress response pathways were all down-regulated in the presence of SMG. In contrast, a cluster of seven metallothionein genes were up-regulated through all the time points. Moreover, HLA-G, a key gene that mediates cellular immune suppression effect, was up-regulated during the recovery phase of SMG exposure. Our findings contribute significantly to the knowledge of epidermal response to SMG, which may suggest a mechanism in the whole body response to microgravity, particularly in microgravity-associated immune response suppression, integrated stress response, and tumor progression.

Results

Morphology of HEK001 cells cultured in HARV bioreactors and in conventional 2D cell culture flasks

Monolayer keratinocytes, HEK001 cells, formed small aggregates and spherical cellular morphology (Figure 1C and E) typical for cells cultured in the 3D environment of HARV bioreactors. When the HEK001 cells were removed from the HARV bioreactors after the shorter (3 and 4 d) SMG exposures and then cultured in conventional 2D cell culture flasks for 15 d, the keratinocytes spread out to form monolayer growth indistinguishable from the untreated controls (compare Figure 1A and B with D and F). Cells from the longer (9 and 10 d) SMG exposures were not recovered as complete as the shorter ones, and elongated cells were found in the recovery culture after 16 d (Figure 1G and H). Figure 1G shows cells after 7-day recovery from a 9-day SMG treatment; note that cell aggregates were visible at the early recovery stage. Although these cells regained their morphological

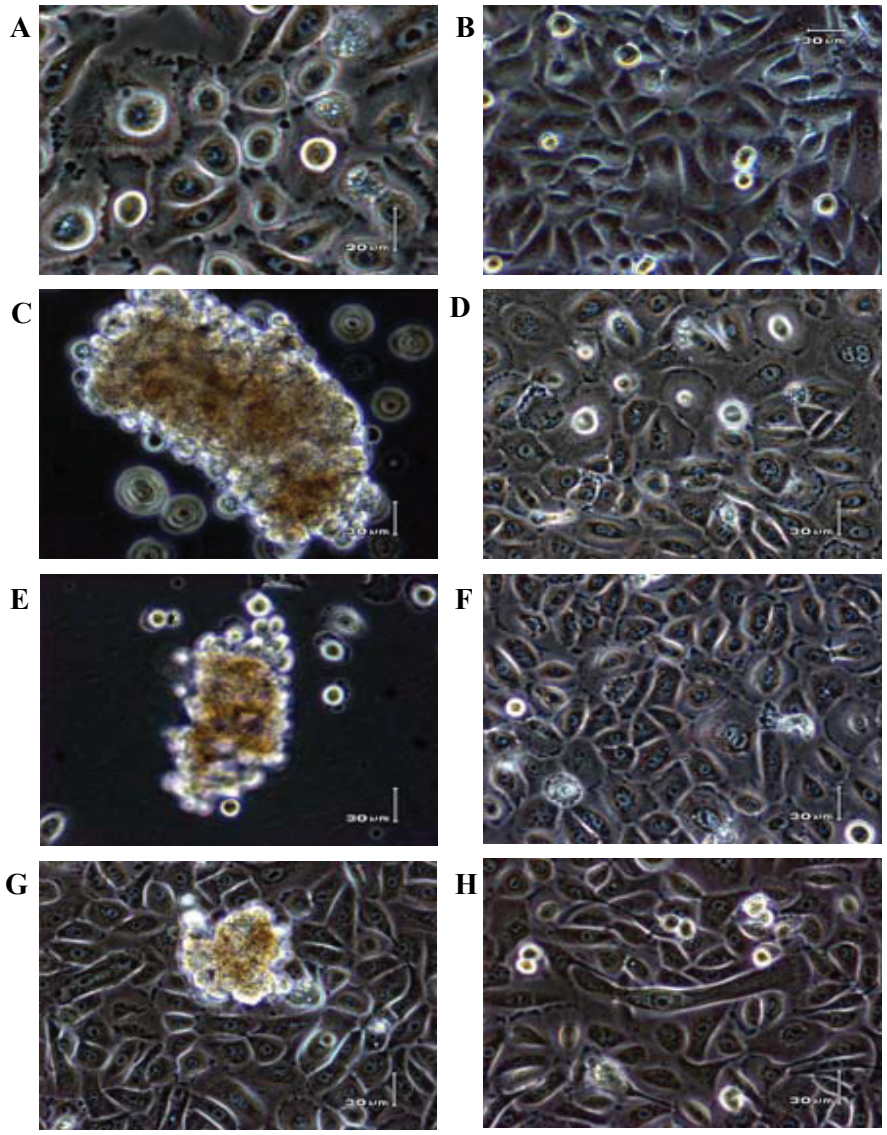

Fig. 1 Morphology of HEK001 cells cultured in HARV bioreactors for SMG treatment and in conventional 2D cell culture flasks for normal gravity recovery. **A** and **B**. HEK001 cells cultured in normal gravity tissue culture flasks showing different photo fields and magnifications of the control cells. **C**. Cell aggregates from 3-day SMG culture. **D**. Cells recovering from 3-day SMG treatment in Panel C by 15-day growth in normal (1 *g*) gravity (culture flasks). **E**. Cell aggregates from 4-day SMG treatment. **F**. Cells recovering from 4-day SMG treatment through 15-day culture in normal gravity. **G**. Cells after 7-day recovery in normal gravity from 9-day SMG treatment. **H**. Cells after 16-day recovery in normal gravity from 10-day SMG treatment.

appearance after extended culturing under normal gravity, the extent to which cellular gene activity was affected by the SMG treatments and whether the altered gene functions would ever recover were of crucial interest. Therefore, we next investigated through DNA microarray analysis for genome-wide gene expression evaluation and through Northern blotting for gene-specific validation.

General gene expression profiles and distributions of the time course microarray data

To visualize the general gene expression profiles of the microarray data, we first plotted the extracted microarray data in MA plots (Figure 2). In the MA plots, each point represents one feature from a corre-

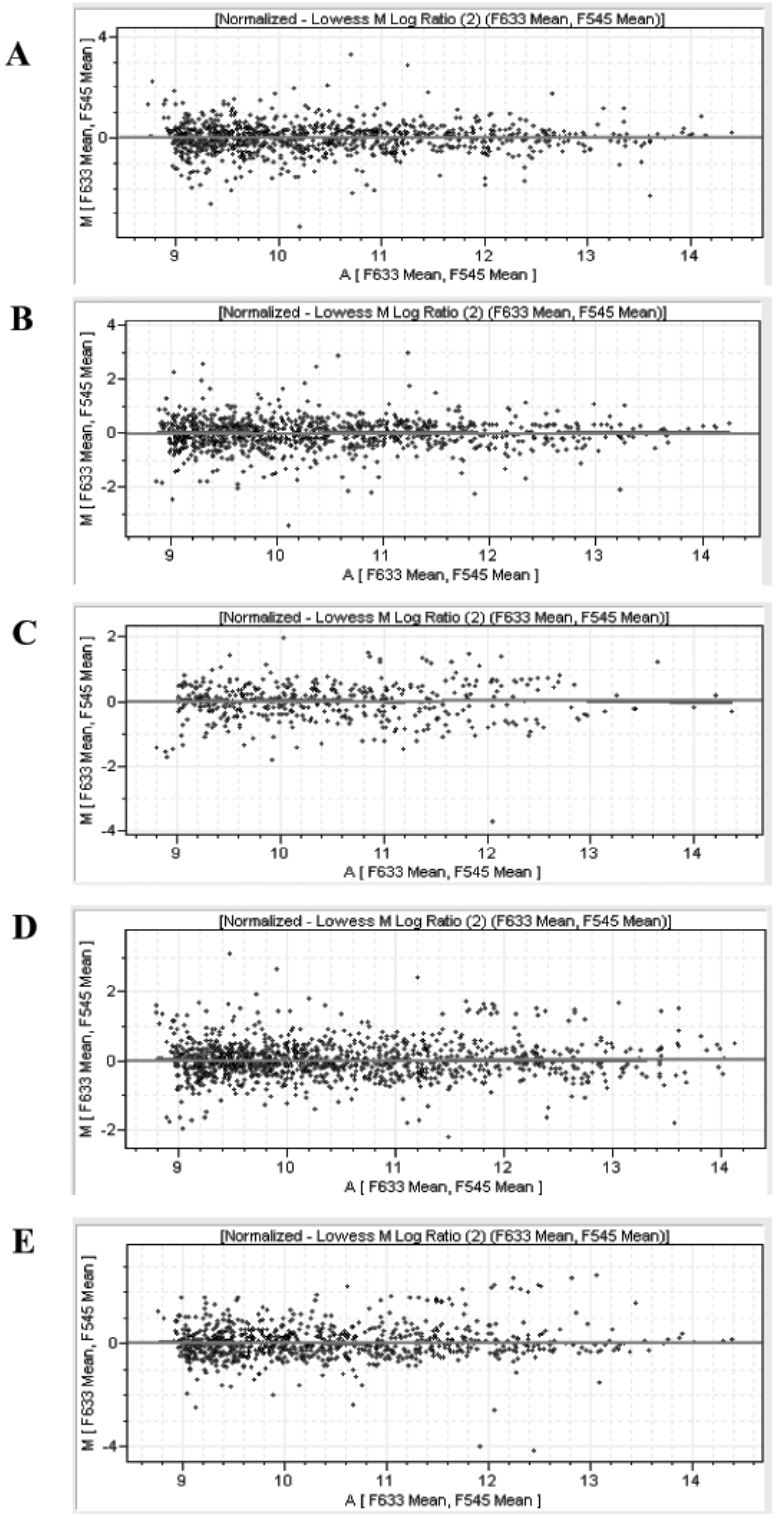

Fig. 2 MA scatter plots showing the average trend of the log ratio as a function of intensity of features in Arrays 1–5 using Lowess normalization. Each point represents one feature from the corresponding microarray. F633 represents the intensity of the red (R) laser wavelength (633 nm) that excites the cyanine 5 dye. F545 represents the intensity of the green (G) laser wavelength (545 nm) that excites the cyanine 3 dye. The MA plot shows the log intensity ratio M= $\log_2(R/G)$ versus the average intensity A= $\frac{1}{2}(\log_2 R+\log_2 G)$. **A**. MA plot for 3-day SMG (Array 1). **B**. MA plot for 4-day SMG (Array 2). **C**. MA plot for 4-day SMG followed by 15-day recovery at 1 *g* (Array 3). **D** and **E**. MA plots for 9-day and 10-day SMG followed by 50-day and 60-day recovery at 1 *g*, respectively (Arrays 4 and 5).

sponding microarray. The plots of five different microarray experiments before and after normalization show the general gene expression profiles of the cells exposed to different doses of SMG and during different recovery periods (Arrays 1–5; Figure 2A–E). After normalization and statistical analysis (student t-test) of the microarray data, a total of 314 differentially regulated genes from the five time course microarrays were identified as statistically significant ($p \leq 0.05$). We further filtered the 314 genes to a cut-off point of 1.5-fold up- or down-regulation. Thus, a total of 162 genes were identified from the five SMG experiments to be significantly ($\geq$1.5-fold change, $p \leq 0.05$) differentially expressed, constituting the initial pool of the putative gravity sensitive genes in the SMG-treated keratinocytes (see Table 1 in Appendix). The numbers of differentially regulated genes allocated for each of the five (Arrays 1–5) microarrays were 101, 94, 18, 105, and 86, respectively. These putative gravity sensitive genes of the keratinocytes were subjected to further bioinformatics analysis.

Functional grouping and time course expression profiles of the 162 gravity sensitive genes

The significantly differentially expressed genes in each of the five experiments were further categorized into 18 functional groups using histograms as shown in Figure 3. For each experiment, the number of genes induced (red) and suppressed (blue) was graphed for each of the 18 functional categories, generating an individual histogram profile for the corresponding microarray. Figure 3A shows the functional distribution of 101 SMG-affected genes exposed to 3-day microgravity (Array 1) with 34 induced and 67 suppressed. Those exposed to 4-day SMG (Array 2) exhibited a similar expression pattern, with 32 genes up-regulated and 62 down-regulated (Figure 3B). In contrast, the cells that were cultured for 4-day SMG and then recultured and grown at 1 g for 15 d recovered from the microgravity effect more efficiently, with only 18 genes exhibiting significant differential regulation (10 up and 8 down) (Figure 3C). The cells that were grown in SMG for 9 and 10 d followed by recovery culturing at 1 g for 50 and 60 d, respectively, exhibited a similar expression pattern to each other and to the first two time points (compare Figure 3D and E with A and B). The effect of the longer exposures followed by the near two-month recovery time seemed to be equivalent to the shorter exposures without recovery. Most notably across the four similar profiles (Figure 3A, B, D, E), cellular functions affected by SMG mainly were metabolism, cell communication, cell development, and cell death. The data suggest a critical role of the recovery growth in mitigating the alteration of cellular gene functions from prolonged SMG exposure. The recovery effect was even more apparent in Array 3 (Figure 3C), which showed that only 18 genes were differentially expressed compared with the non-treated control, while >80% of the genes had returned to homeostasis after 15-day recovery in normal gravity.

Cluster analysis of genes differentially expressed under microgravity and recovery

The 162 differentially regulated genes were clustered hierarchically into five clusters (Figure 4; Table 1) using average-linkage clustering (*33*). Cluster I was coordinately down-regulated, consisting of 14 genes, 11 of which were from the integrated stress response pathway. The genes in Cluster I from the cells cultured for 3 d (Array 1) and 4 d (Array 2) in SMG were on average down-regulated ~3.8 fold. When allowed to recover at 1 g for 15 d (Array 3), >80% of these genes recovered to non-exposed level. The genes that were exposed to SMG for 9 and 10 d and were allowed to recover at 1 g for 50 d (Array 4) and 60 d (Array 5), respectively, showed a level of down-regulation similar to those exposed to SMG for 3 and 4 d. Cluster II has 83 genes. The expression pattern was very similar between 3-day and 4-day SMG, with the average down-regulation of ~1.7 fold, and similar between 9-day and 10-day SMG followed by 50-day and 60-day recovery at 1 g, respectively, with the average down-regulation of ~1.5 fold. This cluster did not show significant differential expression after exposure to 4-day SMG followed by 15-day recovery at 1 g. There are 17 genes represented in Cluster III. The average expression level for 3-day and 4-day SMG exposure was ~2 fold. Again, this cluster did not show significant differential expression after exposure to 4-day SMG followed by 15-day recovery. Cluster IV is comprised of eight metallothione genes that were all up-regulated across the five time points. The level of up-regulation was ~2 fold across the first three time points. After 9-day SMG followed by 50-day recovery, the Cluster IV gene expression increased to ~4-fold

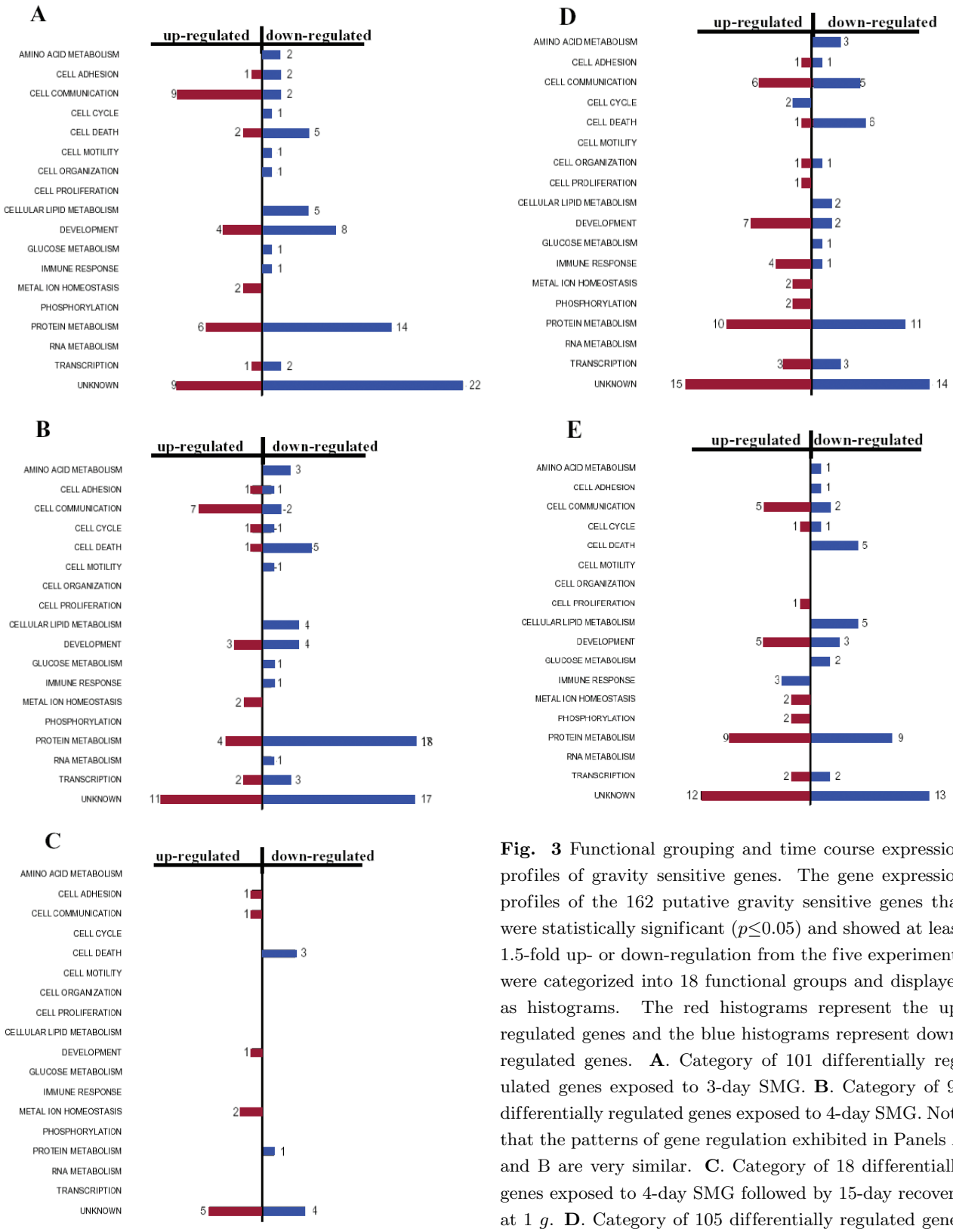

Fig. 3 Functional grouping and time course expression profiles of gravity sensitive genes. The gene expression profiles of the 162 putative gravity sensitive genes that were statistically significant ($p \leq 0.05$) and showed at least 1.5-fold up- or down-regulation from the five experiments were categorized into 18 functional groups and displayed as histograms. The red histograms represent the up-regulated genes and the blue histograms represent down-regulated genes. **A**. Category of 101 differentially regulated genes exposed to 3-day SMG. **B**. Category of 93 differentially regulated genes exposed to 4-day SMG. Note that the patterns of gene regulation exhibited in Panels A and B are very similar. **C**. Category of 18 differentially genes exposed to 4-day SMG followed by 15-day recovery at 1 *g*. **D**. Category of 105 differentially regulated genes exposed to 9-day SMG followed by 50-day recovery. **E**. Category of 95 differentially regulated genes exposed to 10-day SMG followed by 60-day recovery.

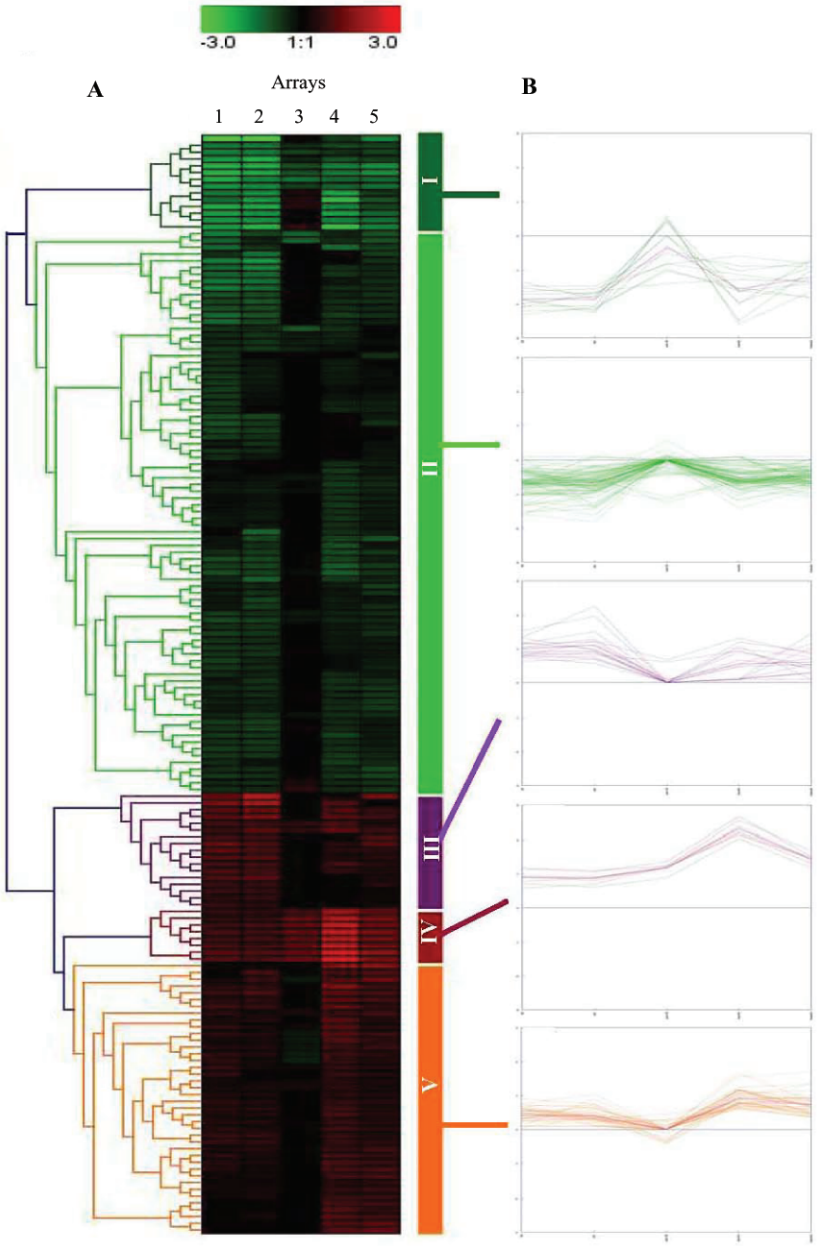

Fig. 4 Cluster analysis of 162 differentially regulated genes from five microarray experiments showing the trend in time course. **A**. The average-linkage hierarchal clustering of the expression data ($\log_2$) of all the 162 significant genes. The rows represent individual genes categorized into five hierarchical clusters according to differential expression levels. The columns represent the five microarray experiments showing the gene expression pattern for each time point according to the five clusters. **B**. The time course trend of expression of all of the genes represented in each cluster.

up-regulation. After 10-day SMG followed by 60-day recovery, however, the Cluster IV gene expression returned to the level similar to the levels of the shorter exposure time points (∼2-fold up-regulation). It may be that an additional 10 more days' recovery time was needed to allow the longest exposed cells to recover to the impact level of shorter exposed cells. In Cluster V (40 genes), there was an average up-regulation of ∼1.5 fold after 3-day and 4-day SMG and a drop to little (no differential regulation or complete recovery) after 15-day recovery. However, for 9-day and 10-day SMG followed with recovery at 1 g for 50 and 60 d, it showed a similar expression pattern (∼1.6-fold up-regulation) to those cultured under SMG for 3 and 4 d. Thus, the close to two-month recovery time again reduced the SMG effect to the level of shorter exposures for the 40 genes in this cluster.

Overlapping patterns of differentially expressed genes among the five SMG experiments and the identification of "center genes"

When comparing Arrays 1 and 2 for the 3-day and 4-day SMG (Figure 5A) using the Venn diagram, we found that a total of 76 differentially regulated genes (27 up and 49 down) were common to both microarrays, showing a consistency of ~75% between the two different time points. A total of merely 18 differentially expressed genes in Array 3 indicated that >80% of the genes had recovered from the 4-day microgravity effect after 15 d in normal gravity culture. Out of these 18 significant genes, there were 17 and 16 genes shared with the 3-day and 4-day microgravity treatment alone, respectively; this constituted about 90% of all the significant genes identified from Array 3. The data suggest a causal link for the remnant SMG affected genes, which resulted from having not yet completely recovered from the SMG treatment. Figure 5B allowed us to further compare the expression patterns between the shorter exposures alone and the longer exposures followed with up to a two-month recovery period (Arrays 4 and 5). We found a significant overlap of the differentially regulated genes among the four different time points. Similar to the two shorter exposures (3-day and 4-day SMG) shown

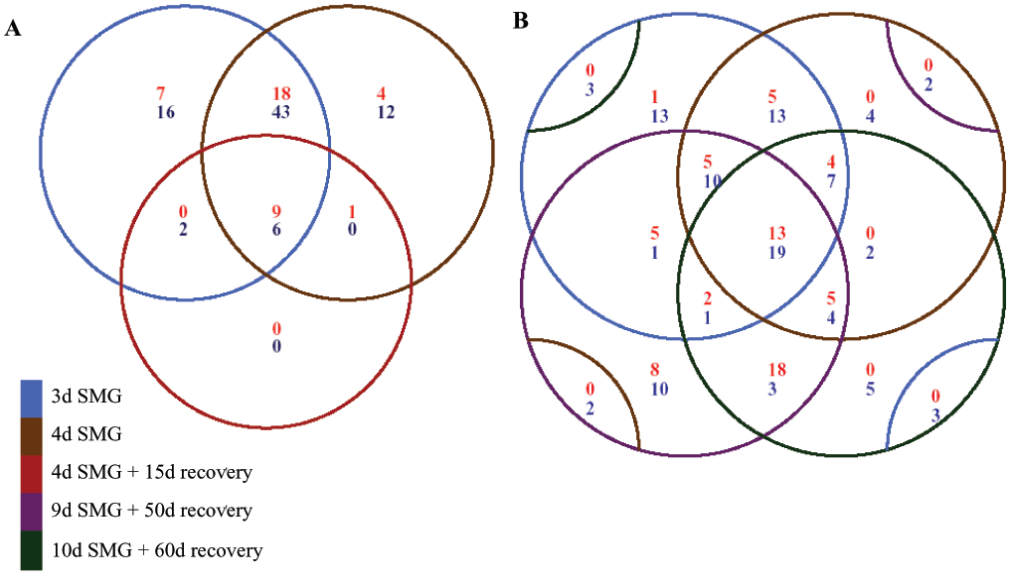

C

1	-11.43	-10.72	-1.73	-3.25	AREG
2	-4.98	-4.25	-2.87	-3.49	HSPA5
3	-4.61	-4.44	-3.04	-3.52	HERPUD1
4	-4.28	-3.12	-2.42	-2.50	PDIA4
5	-4.18	-4.17	-3.14	-1.88	PCK2
6	-3.95	-3.42	-3.87	-2.37	IARS
7	-3.68	-3.46	-3.05	-2.63	SDF2L1
8	-3.68	-4.76	-5.98	-3.09	TRIB3
9	-3.64	-4.55	-2.04	-1.69	SREBF1
10	-3.26	-3.21	-2.20	-2.59	TRA1
11	-2.87	-3.32	-3.99	-1.59	ASNS
12	-2.78	-2.77	-1.83	-1.85	ARMET
13	-2.51	-2.09	-1.73	-1.55	FKBP2
14	-2.53	-3.63	-5.59	-2.00	PHGDH
15	-2.51	-1.55	-2.67	-1.75	PYGB
16	-2.03	-1.82	-2.28	-1.57	HSPA9B
17	-1.79	-1.88	-2.24	-1.70	GHITM
18	-1.52	-1.77	-1.96	-1.63	CDH1
19	-1.51	-1.52	-1.51	-1.95	DHCR7
20	1.64	1.52	4.11	2.26	MT1A
21	1.66	1.56	1.71	1.52	TUBB3
22	1.69	2.06	2.21	1.98	TXN
23	1.72	1.84	5.00	2.70	MT1B
24	1.73	2.34	2.48	1.80	TMEPAI
25	1.86	1.69	2.23	1.58	VAT1
26	1.87	1.84	4.68	2.68	MT1H
27	1.88	1.76	4.54	2.48	MT1X
28	1.92	1.88	5.23	2.71	MT1G
29	2.19	2.32	2.02	1.67	CITED4
30	2.21	2.09	6.38	2.86	MT2A
31	2.22	2.85	2.3	1.87	PLAU
32	2.26	2.14	5.95	3.2	ENST00000245185

Fig. 5 Venn diagrams of overlapping gene expression patterns of the 162 significant genes across the five time points. The red numbers represent up-regulated genes and the blue numbers represent down-regulated genes. **A**. Comparison of gene expression data of 3-day and 4-day SMG exposure with 4-day SMG exposure followed by 15-day recovery at 1 *g*. **B**. Comparison of gene expression data of 3-day and 4-day SMG exposure with 9-day SMG followed by 50-day recovery and 10-day SMG followed by 60-day recovery. The center of the Venn diagrams shows that there are 32 differentially regulated genes between all four array experiments. **C**. Heat map of the expression pattern for the 32 differentially regulated genes identified from the center of the Venn diagrams in Panel B.

in Figure 5A, the two longer exposures (plus longer recovery) shared ∼69% common differentially expressed genes. An important function of the Venn diagram is that it allowed us to readily identify the genes affected by all the SMG treatments through the center of the diagrams: all four time point microarrays shared 32 genes (13 up and 19 down) that are differentially regulated by at least 1.5 fold (Figure 5B and C). These "center genes" were the best candidates for the "major space genes" because they were most consistently affected by SMG.

Validation of microarray results through Northern blotting analysis of ten cellular genes

We also performed Northern hybridization to verify the results from the microarray analysis of the SMG time course experiments. The uniqueness of Northern blotting analysis is that it measures the abundance as well as the size of the RNA of interest (*34*). Figure 6 shows the size identity and expression levels for ten genes, nine of which were significant genes identified through microarray experiments, and GAPDH was used as an internal control. The Northern hybridization reactions were performed sequentially with the ten cDNA probes as shown in the figure. All the hybridizations shown in the figure resulted in one predominant band of the expected sizes (marked with arrows) for the particular mRNAs. However, some minor bands were visible in a few panels. For the TRIB3 probe, the level of the larger band (∼2,500 to 2,800 bp) was down-regulated in SMG; the expression level for another isoform (alternatively spliced) of TRIB3 mRNA (Figure 6C) did not seem to be affected by SMG. There was a higher band found in lanes 1, 4, and 5 of Figure 6G (MT1A probe), which most likely resulted from the incomplete stripping of the TRA1 probe hybridized immediately prior to the hybridization of MT1A.

The bands of the expected sizes for the probed mRNA (marked with arrows) were subjected to quantitative analysis. To quantitatively analyze the mRNA levels from the Northern blots, we first normalized all the mRNA bands in Figure 6A–J against the GAPDH level in each corresponding lane. The normalized levels of the mRNA in each panel were then plotted in histograms as shown in Figure 7. The overall Northern blotting results demonstrated a remarkable resemblance to those obtained from microarray analysis, with an overall high level of correlation between the results from the two methods (R=0.86; Figure 7). The mRNA levels for genes PDIA4, TRIB3, AREG, TRA1, PCK2, and ARMET were shown to be decreased significantly by both microarray analysis and Northern blotting, with correlation coefficient values of 0.97, 0.84, 0.98, 0.69, 0.91, and 0.93, respectively. The MT1X, MT2A, and MT1A mRNA levels were found to be significantly increased by both microarray and Northern blotting analysis, with correlation coefficient values of 0.58, 0.85, and 0.97, respectively. The overall high level of correlation (R=0.86) between the analytical results from microarray and Northern blotting further validated our genome-wide analysis using the microarray technology.

Discussion

Microgravity effects have been closely associated with bone loss, muscle atrophy, and decreased immune function of astronauts. Consequently, extensive studies on cells of the bone, muscle, and blood origin have been documented in literature (*18–20*). Since astronauts experience whole body exposure to microgravity, all the organ systems in the body are potentially affected by the gravity change and may function differently to counterbalance the microgravity stress. The different organ systems may react differently to gravity change. It is also possible that a common set of genes in different cell lineages are preferentially altered in microgravity conditions. To fully understand the microgravity effect on human health, it is important to study the microgravity response of cells of various organ origins. The identification of the common set of gravity sensitive genes may lead to the identification of "major space genes" that together play a major check-and-balance role ultimately determining the outcome of a cell, or an organism such as an individual person, in the response to microgravity conditions.

The gene expression profiles for the five time points were achieved mainly from the 18 functional groups of genes in histograms and hierarchical cluster analysis of all the 162 significantly differentially regulated genes. The nearly identical expression profiles between the 3-day and 4-day SMG treatment indicated a high level of consistency in the number and type of gravity sensitive genes between the closely spaced time points (Figure 3A and B). Similar expression profiles were also found between longer time

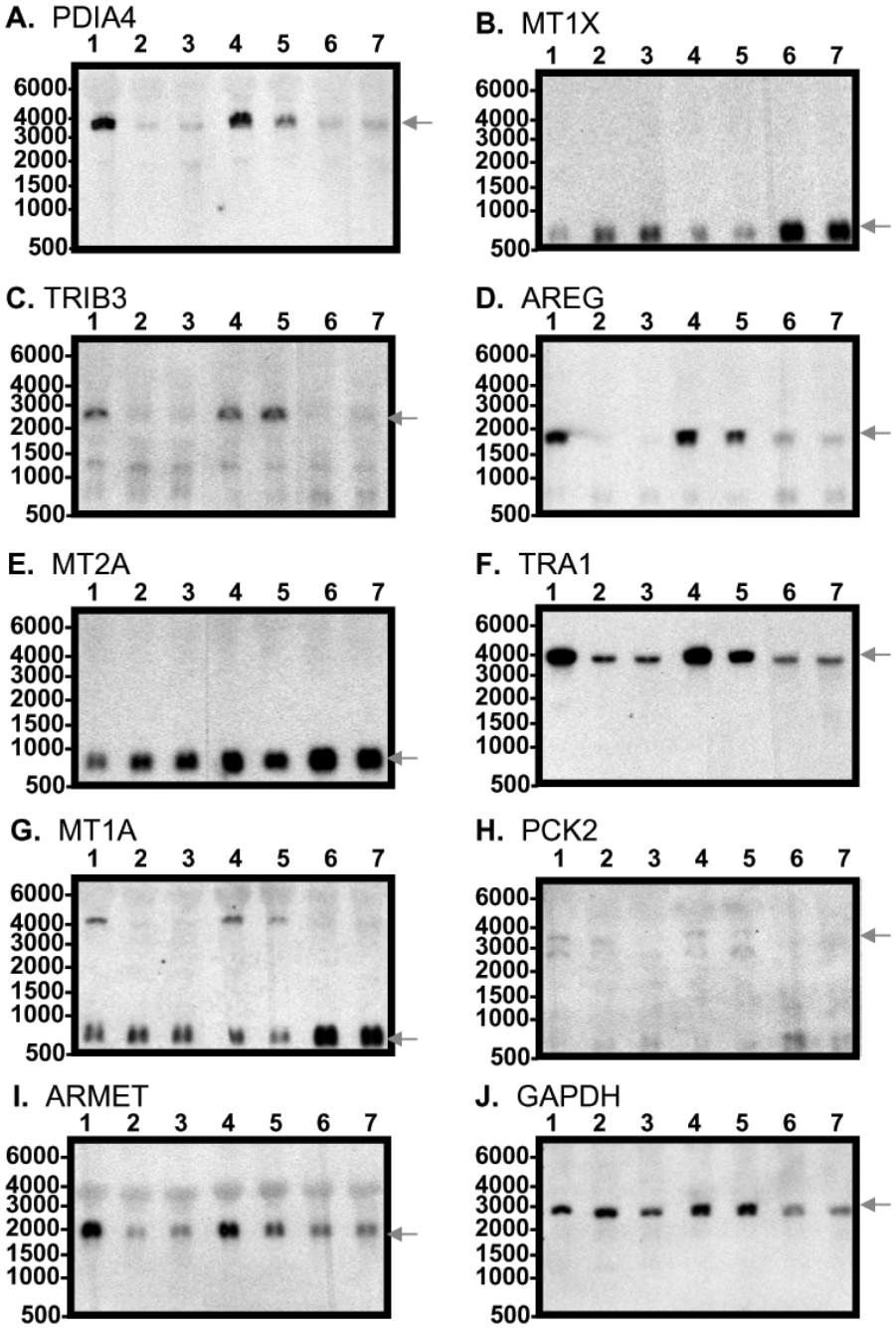

Fig. 6 Validation of microarray results using Northern blotting analysis of genes differently expressed under modeled microgravity conditions. An amount of 10 μg total RNA from each sample was loaded onto a 1% formaldehyde agarose gel. Lanes 1–7 were loaded with samples as the following: Lane 1, conventional stationary control; Lane 2, three-day modeled microgravity; Lane 3, four-day modeled microgravity; Lane 4, three-day microgravity recovery; Lane 5, four-day microgravity recovery; Lane 6, nine-day microgravity recovery; Lane 7, ten-day microgravity recovery. The Northern blot was sequentially hybridized with ten different probes as indicated in Panels A–J: **A**. PDIA4; **B**. MT1X; **C**. TRIB3; **D**. AREG; **E**. MT2A: **F**. TRA1; **G**. MT1A: **H**. PCK2; **I**. ARMET; **J**. GAPDH. The expected mRNA band for each probe was indicated with an arrow to the right side of each panel.

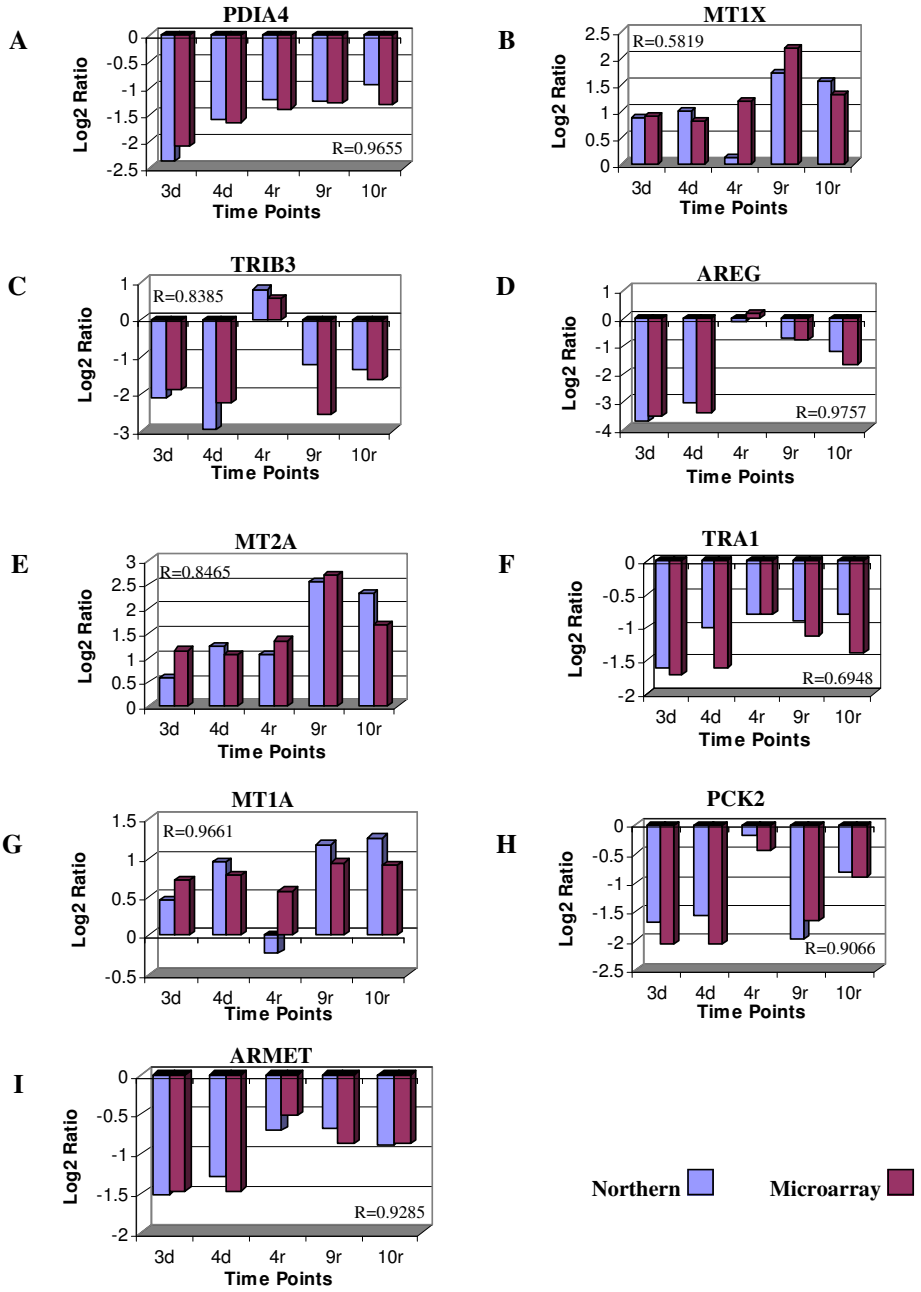

Fig. 7 Quantitative comparison of gene expression data obtained from Northern blotting analysis and microarray analysis. The mRNA bands in Figure 6A–J were first normalized against the GAPDH level in each corresponding lane. The normalized levels of the mRNA in each panel were then plotted in histograms as shown in Figure 7A–I. In the histograms, the Northern blotting data (blue) were plotted side by side with the microarray data (red) to directly compare the expression levels of the same nine significant genes. The values of the correlation coefficient (R values) for each comparison were indicated in each panel.

points, that is, cells recovering from 9-day and 10-day SMG treatment in normal gravity for 50 and 60 d, respectively (Figure 3D and E). The validity of the microarray data was further confirmed with Northern blotting analysis of ten genes (Figures 6 and 7). For SMG exposure time as short as 4 d, a 15-day recovery period resulted in >80% of the SMG affected gene expression returning to homestasis (compare Figure 3C with B). A two-month recovery period mitigated the affected gene expression profile to that equivalent to the 4-day SMG exposure level. Thus, our expression profiling results suggest that the time duration of

microgravity exposure as well as post-SMG recovery are critical determinants of the extent to which cellular gene expression is affected by SMG. The shorter the SMG exposure and the longer the recovery time, the better the recovery from the SMG stress. Based on our results, it is advisable that shorter mission duration time and longer recovery interval would be beneficial to astronauts' health.

We further identified 32 "key" or "center" gravity sensitive genes from the 162 significantly differentially regulated genes detected from the time course experiments. This was achieved by the use of Venn diagrams of the shorter SMG exposures (3-day and 4-day SMG) and the longer exposures (9-day and 10-day SMG followed by 50-day and 60-day recovery) locating the genes that were in the very center of the four interlinked time points (Figure 5B and C). These genes were considered to be most consistently impacted by the microgravity treatment because they were affected by all the interlinked time points of the SMG exposures. These key gravity sensitive genes may be candidates for the "major space genes" whose activities were most significantly affected by the SMG environmental factor and most likely play a determinant role coordinately on the outcome of the SMG exposure effects. Many of these genes were found to be coordinately regulated in specific clusters belonging to particular pathways and are known to be coordinately regulated in non-space environment. One of the most notable groups of coordinately regulated genes was the eleven "center genes" (AREG, HSPA5, HERPUD1, PDIA4, PCK2, SDF2L1, TRIB3, SREBF1, TRA1, ASNS, and ARMET) that all came from Cluster I and were all down-regulated in SMG (Figure 5C; Table 1). These genes are known to be coordinately regulated in integrated stress response pathways such as the endoplasmic reticulum (ER) stress response pathway and the amino acid starvation response pathway (*35*, *36*). They are typically induced coordinately in the presence of ER stress or in response to amino acid starvation (*35*, *36*). It is not clear why these genes were all down-regulated under reduced gravity conditions. It maybe that microgravity is favorable for protein folding and transport, making the machinery for the ER protein unfold stress response pathway unnecessary. To our knowledge, this is the first report to connect this set of integrated stress response genes to microgravity response. Nonetheless, in a study comparing the gene expression from cells grown in microgravity on the space shuttle with those grown in SMG, TRA1 was found to be down-regulated for 5.5 fold and 1.2 fold, respectively (*37*). In agreement with the reported space shuttle and SMG results, TRA1 in our experiment was also down-regulated across all the time points (from ∼3.2 fold to ∼1.75 fold) in SMG. TRA1 has also been found to be up-regulated in a variety of tumor cells in response to glucose depletion, hypoxia, and decreased pH. Therefore, TRA1 seems to be implicated in cell immunity against cancer cells (*38*).

Another group of coordinately regulated genes that were also found in the center of the four interlinked time points includes seven metallothionein genes (MT1A, MT1B, MT1G, MT1H, MT1X, MT2A, and a MT2A clone ENST00000245185) in Cluster IV. These genes were all major isoforms of metallothioneins and were up-regulated in all the SMG time points, even more significant during recovery periods (Figure 4 and Figure 5C; Table 1). Consistent with our result, MT1A and MT2A expressions have been found to be up-regulated in space-flown (16 d) rat skeletal muscles (*20*). MT-I and MT-II isoforms have very similar structures and functions and are coordinately regulated in most cells (*39*, *40*). They have cellular functions primarily in metal ion homeostasis, scavenging of ROS, redox status, immune defense responses, cell proliferation, and cell death (*40*, *41*). MT-I and MT-II are induced by most inflammatory or pathological stimulus such as proinflammatory cytokines and oxidative stress (*42*). In addition, our microarray data showed several genes involved in immune response such as HLA-G and IL-1β to be affected by SMG (Table 1, Cluster V). Although IL-1β induction has been reported in a macrophage cell line in space (*43*), it is not known whether HLA-G gene expression would be altered by microgravity. In normal gravity environment, HLA-G has been shown to have direct inhibitory effect on T, APC, and NK cell functions in the immune system and induces suppressor T-cells. HLA-G also plays a role in tumor-driven immune escape mechanism of cancer cells during the later phase in host and tumor cell interactions (*44*). Our finding that HLA-G mRNA levels were up-regulated in microgravity-exposed keratinocytes may suggest an underlining mechanism for microgravity-associated immune response suppression.

Conclusion

In summary, our results indicated that cellular gene activity achieved >80% recovery from the shorter ex-

posure time (≤4 d) in a recovery period of 15 d, while a longer recovery period (≥50 d) was needed for genes to recover to the shorter exposed impact levels after an exposure time as long as 9 and 10 d. Interestingly, a cluster of eleven genes in the integrated stress response pathway that are inducible by ER stress and amino acid starvation were all down-regulated in the presence of SMG. In contrast, a number of genes involved in proliferation, development, and cancer were up-regulated. A cluster of seven metallothionein genes were all up-regulated through all the time points. In addition, HLA-G, a key gene that mediates cellular immune suppression effect, was up-regulated during recovery phases of SMG exposure. Our findings contribute significantly to the knowledge of epidermal response to SMG, which may suggest a mechanism in the whole body response to microgravity, particularly in microgravity-associated immune response suppression, integrated stress response, and tumor progression. Overall, the data suggests, for health's sake, shorter mission duration in space may lead to quicker and more complete recovery from the microgravity effects.

Materials and Methods

Cell culture

HEK001, an immortalized human skin keratinocyte cell line of basal-like type (*45*), was purchased from American Type Culture Collection (Manassas, VA, USA) and cultured at 37°C with 95% humidity and 5% CO_2 in Ketatinocyte-Serum Free medium with 5 ng/mL human recombinant EGF, 50 ug/mL bovine pituitary extract, and 2 mM L-glutamine.

Simulated microgravity and cell exposure

Ground-based modeled microgravity was achieved using the 50 mL HARV units of the rotating wall vessel (RWV) culture apparatus (a NASA JSC invention) from Synthecon, Inc (Houston, TX, USA). Cell viability and cell concentration were determined by Vi-Cell 1.01 cell counter of Beckman Coulter (Fullerton, CA, USA). For the 3-day and 4-day modeled microgravity exposures, a density of 2.0×10^5 cell/mL with viability of 93.2% of the HEK001 cells were cultured in RWV bioreactors at 17.2 rpm to achieve the constant free-fall experience for cell aggregates. At the end of the 3-day and 4-day microgravity exposure, the contents of the bioreactor vessels were poured out into a 50 mL sterile centrifuge tube to collect cell pellets, and 5 mL of the cell suspension from the bioreactor vessels was transferred to T75 flasks for morphological observation and for further stationary culture. Hence, the recovery stage for the exposed cells as well as post 3-day and post 4-day microgravity recovery cell samples were achieved. After the removal of the cells from the vessels, fresh medium was used to refill the vessels for extended microgravity exposure to 9 and 10 d, respectively. The resulted cells were all transferred to stationary culture for recovery of 50 and 60 d, with medium change twice per week. Non-exposed stationary controls and the recovery stage of microgravity-exposed HEK001 cells were cultured in tissue culture flasks with vented caps (TPP Techno Plastic Products, Trasadingen, Switzerland) in the same incubator at 37°C with 5% CO_2.

Total RNA isolation and DNA microarray hybridization

HEK001 cells cultured in modeled microgravity HARV bioreactors and control flasks were removed at their respective time points, washed with PBS for three times and lysed in guanidinium isothiocyanate buffer. The cell lysates were stored at −80°C prior to ultracentrifugation for total RNA isolation (*46*, *47*). Total cellular RNA was labeled using the Agilent Low RNA Input fluorescent Linear Amplification Kit (Agilent Technologies, Santa Clara, CA, USA) following the manufacturer's protocols (*48*). The fluorescently labeled cRNA probes were further purified and hybridized to Agilent 22K Human Microarray V2 according to the specified procedures within the kit.

Microarray scanning, feature extraction, and functional grouping

The microarrays were scanned using a ScanArray microarray scanner (Perkin-Elmer, Waltham, MA, USA). The images generated from the scanning were imported into GenePix 6.0 (Molecular Devices, Sunnyvale, CA, USA) for alignment and initial quantitation. Lowess normalization and some statistical analyses were performed in Acuity 4.0 (Molecular Devices). The normalized genes were then subjected to a student t-test to determine statistical significance. An alteration in gene expression level was considered significant if it passed a statistically significant level of $p \leq 0.05$ and met the minimum cut-off of 1.5-fold

differential regulation. The significant genes thus identified were further processed using EASE (*49*) to identify 18 functional categories and relevant pathways. The functional categories were then used to organize the gene table (Table 1) and to generate the comparative histograms (Figure 3).

Hierarchical clustering and Venn diagrams

We also used the average-linkage hierarchical clustering to better organize and visualize the expression patterns in the data (*33*, *50*). The hierarchical clustering was performed using Genesis 1.0 (*51*). To more easily identify the genes affected by all the SMG treatments, we generated Venn diagrams using AFM 4.0 (*52*).

Northern blotting, normalization, and quantitative analysis

Some of the significantly regulated microgravity sensitive genes identified from the DNA microarray analysis were further verified using Northern blotting. Briefly, 10 μg total RNA was loaded per lane on a 1% formaldehyde agarose gel for electrophoresis separation of RNA species. The gel-separated RNAs were capillarilly transferred onto a nylon membrane, which was subjected to a hybridization procedure using chemilluminascently (Pierce Biotechnology, Rockford, IL, USA) labeled cDNA probe fragments. The blot was sequentially hybridized with ten different probe fragments. The cDNA probe fragments were generated from RT-PCR reactions using total cellular RNA as the templates. RT-PCR reactions were carried out to generate the cDNA probes required for the Northern blotting analysis, using the Reverse Transcription System of Promega (Madison, WI, USA) and the Bio-Line Red DNA Polymerase PCR kit (Taunton, MA, USA). For Northern blot quantitation, the autoradiographs of the Northern blots were scanned and saved as TIF images for further analysis. The images were then opened in Unscan-It Gel (Silk Scientific, Orem, UT, USA) for quantitation. To quantitatively analyze the mRNA levels from the Northern blots, we first normalized the mRNA bands in Figure 6A–J against the GAPDH level in each corresponding lane. The normalized levels of the mRNA in each panel were then plotted in histograms as shown in Figure 7.

Acknowledgements

We thank the NASA University Research Center for Biotechnology and Environmental Health at Texas Southern University for discussion and support. We are especially grateful for the encouragement and support provided by the Technical Review Group of NASA Johnson Space Center. This work was funded by NASA JSC Grant No. NCC9-165 and NIH Grant No. RR03045-12A1.

Authors' contributions

JQC conceived and supervised the project, collected the data, conducted the data analysis, and prepared the manuscript. SML assisted with data collection and analysis. BLW supervised all the URC projects. All authors read and approved the final manuscript.

Competing interests

The authors have declared that no competing interests exist.

References

1. Leach, C.S., *et al.* 1990. Medical considerations for extending human presence in space. *Acta Astronaut.* 21: 659-666.
2. Cogoli, A. 1993. The effect of hypogravity and hypergravity on cells of the immune system. *J. Leukoc. Biol.* 54: 259-268.
3. Cogoli, A., *et al.* 1993. Mitogenic signal transduction in T lymphocytes in microgravity. *J. Leukoc. Biol.* 53: 569-575.
4. Fritsch-Yelle, J.M., *et al.* 1996. Microgravity decreases heart rate and arterial pressure in humans. *J. Appl. Physiol.* 80: 910-914.
5. Atkov, O.Yu. 1992. Some medical aspects of an 8-month's space flight. *Adv. Space Res.* 12: 343-345.
6. Aubert, A.E., *et al.* 2005. Cardiovascular function and basics of physiology in microgravity. *Acta Cardiol.* 60: 129-151.
7. Hammond, T.G. and Hammond, J.M. 2001. Optimized suspension culture: the rotating-wall vessel. *Am. J. Physiol. Renal Physiol.* 281: F12-25.
8. Nickerson, C.A., *et al.* 2003. Low-shear modeled microgravity: a global environmental regulatory signal affecting bacterial gene expression, physiology, and pathogenesis. *J. Microbiol. Methods* 54: 1-11.

9. Schwartz, R.P., *et al.* 1992. Cell culture for three-dimensional modeling in rotating-wall vessels: an application of simulated microgravity. *J. Tissue Cult. Methods* 14: 51-58.
10. Rucci, N., *et al.* 2002. Characterization of the osteoblast-like cell phenotype under microgravity conditions in the NASA-approved Rotating Wall Vessel bioreactor (RWV). *J. Cell. Biochem.* 85: 167-179.
11. Ontiveros, C., *et al.* 2004. Hypoxia suppresses runx2 independent of modeled microgravity. *J. Cell. Physiol.* 200: 169-176.
12. Patel, M.J., *et al.* 2007. Identification of mechanosensitive genes in osteoblasts by comparative microarray studies using the rotating wall vessel and the random positioning machine. *J. Cell. Biochem.* 101: 587-599.
13. Klaus, D.M. 2001. Clinostats and bioreactors. *Gravit. Space Biol. Bull.* 14: 55-64.
14. Cooper, D., *et al.* 2001. Suppression of antigen-specific lymphocyte activation in modeled microgravity. *In Vitro Cell. Dev. Biol. Anim.* 37: 63-65.
15. Risin, D. and Pellis, N.R. 2001. Modeled microgravity inhibits apoptosis in peripheral blood lymphocytes. *In Vitro Cell. Dev. Biol. Anim.* 37: 66-72.
16. Plett, P.A., *et al.* 2001. Proliferation of human hematopoietic bone marrow cells in simulated microgravity. *In Vitro Cell. Dev. Biol. Anim.* 37: 73-78.
17. Sytkowski, A.J. and Davis, K.L. 2001. Erythroid cell growth and differentiation *in vitro* in the simulated microgravity environment of the NASA rotating wall vessel bioreactor. *In Vitro Cell. Dev. Biol. Anim.* 37: 79-83.
18. Graebe, A., *et al.* 2004. Physiological, pharmacokinetic, and pharmacodynamic changes in space. *J. Clin. Pharmacol.* 44: 837-853.
19. Crawford-Young, S.J. 2006. Effects of microgravity on cell cytoskeleton and embryogenesis. *Int. J. Dev. Biol.* 50: 183-191.
20. Nichols, H.L., *et al.* 2006. Proteomics and genomics of microgravity. *Physiol. Genomics* 26: 163-171.
21. Hatton, J.P., *et al.* 2002. Microgravity modifies protein kinase C isoform translocation in the human monocytic cell line U937 and human peripheral blood T-cells. *J. Cell. Biochem.* 87: 39-50.
22. Walther, I., *et al.* 1998. Simulated microgravity inhibits the genetic expression of interleukin-2 and its receptor in mitogen-activated T lymphocytes. *FEBS Lett.* 436: 115-118.
23. Fitts, R.H., *et al.* 2000. Effect of spaceflight on the isotonic contractile properties of single skeletal muscle fibers in the rhesus monkey. *J. Gravit. Physiol.* 7: S53-54.
24. Lalani, R., *et al.* 2000. Myostatin and insulin-like growth factor-I and -II expression in the muscle of rats exposed to the microgravity environment of the NeuroLab space shuttle flight. *J. Endocrinol.* 167: 417-428.
25. Yamakuchi, M., *et al.* 2000. Type I muscle atrophy caused by micreogravity-induced decrease of myocyte enhancer factor 2C (MEF2C) protein expression. *FEBS Lett.* 477: 135-140.
26. Yu, Z.B., *et al.* 2001. A proteolytic NH_2-terminal truncation of cardiac troponin I that is up-regulated in simulated microgravity. *J. Biol. Chem.* 276: 15753-15760.
27. Carmeliet, G., *et al.* 1998. Gene expression related to the differentiation of osteoblastic cells is altered by microgravity. *Bone* 22: 139S-143S.
28. Hughes-Fulford, M. 2002. Physiological effects of microgravity on osteoblast morphology and cell biology. *Adv. Space Biol. Med.* 8: 129-157.
29. Klein-Nulend, J., *et al.* 2003. Microgravity and bone cell mechanosensitivity. *Adv. Space Res.* 32: 1551-1559.
30. Meyers, V.E., *et al.* 2004. Modeled microgravity disrupts collagen I/integrin signaling during osteoblastic differentiation of human mesenchymal stem cells. *J. Cell. Biochem.* 93: 697-707.
31. Williams, I.R. and Kupper, T.S. 1996. Immunity at the surface: homeostatic mechanisms of the skin immune system. *Life Sci.* 58: 1485-1507.
32. Abbas, A.K., *et al.* 1994. *Cellular and Molecular Immunology* (second edition), pp. 223-235. W.B. Saunders Company, Philadelphia, USA.
33. Quackenbush, J. 2001. Computational analysis of microarray data. *Nat. Rev. Genet.* 2: 418-427.
34. Sambrook, J. and Russell, D.W. 2001. *Molecular Cloning: A Laboratory Manual* (third edition), Vol. 1, 7.21. Cold Spring Harbor Press, New York, USA.
35. Ni, M. and Lee, A.S. 2007. ER chaperones in mammalian development and human diseases. *FEBS Lett.* 581: 3641-3651.
36. Ron, D. and Walter, P. 2007. Signal integration in the endoplasmic reticulum unfolded protein resposnse. *Nat. Rev. Mol. Cell. Biol.* 8: 519-529.
37. Hammond, T.G., *et al.* 2000. Mechanical culture conditions effect gene expression: gravity-induced changes on the space shuttle. *Physiol. Genomics* 3: 163-173.
38. Esseghir, S., *et al.* 2007. Identification of *NTN4*, *TRA1*, and *STC2* as prognostic markers in breast cancer in a screen for signal sequence encoding proteins. *Clin. Cancer Res.* 13: 3164-3173.
39. Searle, P.F., *et al.* 1984. Regulation, linkage, and sequence of mouse metallothionein I and II genes. *Mol. Cell. Biol.* 4: 1221-1230.
40. Penkowa, M. 2006. Metallothionein I+II expression and roles during neuropathology in the CNS. *Dan. Med. Bull.* 53: 105-121.
41. Nath, R., *et al.* 2000. Metallothioneins, oxidative stress and the cardiovascular system. *Toxicology* 155:

17-26.
42. Vasto, S., *et al.* 2006. Inflammation, genes and zinc in ageing and age-related diseases. *Biogerontology* 7: 315-327.
43. Chapes, S.K., *et al.* 1992. Cytokine secretion by immune cells in space. *J. Leukoc. Biol.* 52: 104-110.
44. Rouas-Freiss, N., *et al.* 2007. Expression of tolerogenic HLA-G molecules in cancer prevents antitumor responses. *Semin. Cancer Biol.* 17: 413-421.
45. Sugerman, P.B. and Bigby, M. 2000. Preliminary functional analysis of human epidermal T cells. *Arch. Dermatol. Res.* 292: 9-15.
46. Wilkinson, M.F. 1991. Purification of RNA. In *Essential Molecular Biology: A Practical Approach* (ed. Brown, T.A.), Vol.1, pp. 69-86. Oxford University Press, New York, USA.
47. Clement, J.Q., *et al.* 1999. The stability and fate of a spliced intron from vertebrate cells. *RNA* 5: 206-220.
48. Wolber, P.K., *et al* 2001. The Agilent *in situ*-synthesized microarray platform. *Methods Enzymol.* 410: 28-57.
49. Hosack, D.A., *et al.* 2003. Identifying biological themes within lists of genes with EASE. *Genome Biol.* 4: R70.
50. Eisen, M.B., *et al.* 1998. Cluster analysis and display of genome-wide expression patterns. *Proc. Natl. Acad. Sci. USA* 95: 14863-14868.
51. Sturn, A., *et al.* 2002. Genesis: cluster analysis of microarray data. *Bioinformatics* 18: 207-208.
52. Brietkruetz, B.J., *et al.* 2001. AFM 4.0: a toolbox for DNA microarray analysis. *Genome Biol.* 2: software0001.

Appendix

Table 1 Identification and clustering of 162 putative gravity sensitive genes*

Accession No.	Gene symbol	1#	2#	3#	4#	5#	Gene description	Biological process
CLUSTER I								
NM_001657	AREG	-11.43	-10.72	1.13	-1.73	-3.25	amphiregulin (schwannoma-derived growth factor)	Cell communication
NM_006010	ARMET	-2.78	-2.77	-1.43	-1.83	-1.85	arginine-rich, mutated in early stage tumors	Unknown
NM_001673	ASNS	-2.87	-3.32	1.31	-3.99	-1.59	asparagine synthetase (ASNS), transcript variant 2	Amino acid metabolism
NM_004343	CALR	-3.08	-2.92	-1.77	-1.49	-1.75	calreticulin	Cell cycle
NM_014685	HERPUD1	-4.61	-4.44	-1.94	-3.04	-3.52	homocysteine-inducible, endoplasmic reticulum stress-inducible, ubiquitin-like domain member 1, transcript variant 1	Protein metabolism
NM_004134	HSPA5	-4.98	-4.25	-2.03	-2.87	-3.49	heat shock 70 kDa protein 5 (glucose-regulated protein, 78 kDa)	Cell cycle
NM_013417	IARS	-3.95	-3.42		-3.87	-2.37	isoleucine-tRNA synthetase (IARS), transcript variant long	Protein metabolism
NM_004563	PCK2	-4.18	-4.17	1.37	-3.14	-1.88	phosphoenolpyruvate carboxykinase 2 (mitochondrial), nuclear gene encoding mitochondrial protein, transcript variant 1	Glucose metabolism
NM_004911	PDIA4	-4.28	-3.12	-2.63	-2.42	-2.50	protein disulfide isomerase family A, member 4	Unknown
NM_006623	PHGDH	-2.53	-3.63	1.39	-5.59	-2.00	phosphoglycerate dehydrogenase	Development
NM_022044	SDF2L1	-3.68	-3.46		-3.05	-2.63	stromal cell-derived factor 2-like 1	Unknown
NM_001005291	SREBF1	-3.64	-4.55	-1.30	-2.04	-1.69	sterol regulatory element binding transcription factor 1, transcript variant 1	Cellular lipid metabolism
NM_003299	TRA1	-3.26	-3.21	-1.75	-2.20	-2.59	tumor rejection antigen (gp96) 1	Cell cycle
NM_021158	TRIB3	-3.68	-4.76	1.48	-5.98	-3.09	tribbles homolog 3 (Drosophila)	Unknown
CLUSTER II								
NM_001605	AARS	-1.73	-1.83	-1.01	-1.43	-1.22	alanyl-tRNA synthetase	Protein metabolism
NM_001001937	ATP5A1	-1.64	-1.12	1.04	-1.20	-1.25	ATP synthase, H^+ transporting, mitochondrial F1 complex, alpha subunit, isoform 1	Development
NM_001697	ATP5O	-2.06	-1.93	1.09	-1.39	-1.60	ATP synthase, H^+ transporting, mitochondrial F1 complex, O subunit	Development

Table 1 ***Continued***

Accession No.	Gene symbol	1#	2#	3#	4#	5#	Gene description	Biological process
BC000228	BC000228	-3.02	-1.83	-2.23	-1.41	-2.03	Similar to transducin-like enhancer of split 1, homolog of Drosophila E (sp1)	Unknown
NM_032621	BEX2	-2.86	-2.69		-1.22	-1.57	brain expressed X-linked 2	Unknown
NM_001005266	C15orf21	-2.40	-3.07		-1.58	-1.43	chromosome 15 open reading frame 21, transcript variant 1	Unknown
NM_001009924	C20orf30	-1.71	-1.11		-1.41	-1.35	chromosome 20 open reading frame 30, transcript variant 2	Unknown
NM_000071	CBS	-1.98	-1.93		-1.91	-1.38	cystathionine-beta-synthase	Amino acid metabolism
NM_014550	CARD10	-1.47	-1.38		-1.52	-1.29	caspase recruitment domain family, member 10	Cell cycle
NM_004360	CDH1	-1.52	-1.77		-1.96	-1.63	cadherin 1, type 1, E-cadherin (epithelial)	Cell adhesion
NM_025233	COASY				-1.51	-1.32	Coenzyme A synthase	Unknown
NM_001316	CSE1L	-1.26	-1.62		-1.57	-1.52	CSE1 chromosome segregation 1-like (yeast), transcript variant 1 Cell cycle	
D00022	D00022	-1.57	-1.32	-1.01	-1.33	-1.13	mRNA for F1 beta subunit, complete cds	Unknown
NM_032552	DAB2IP	-1.24	-1.85		-1.33	-1.19	DAB2 interacting protein, transcript variant 1	Unknown
NM_004394	DAP	-1.66	-1.29	1.05	-1.27	-1.13	death-associated protein	Cell cycle
NM_033657	DAP3	-1.23	-1.28	-1.01	-1.61	-1.24	death-associated protein 3	Cell cycle
NM_001919	DCI	-3.00	-3.51			-1.55	dodecenoyl-Coenzyme A delta isomerase (3,2-trans-enoyl-Coenzyme A isomerase), nuclear gene encoding mitochondrial protein	Cellular lipid metabolism
NM_001360	DHCR7	-1.51	-1.52		-1.51	-1.95	7-dehydrocholesterol reductase	Cellular lipid metabolism
NM_006824	EBNA1BP2	-1.56	-1.22		-1.31	-1.09	EBNA1 binding protein 2	Cell organization and biogenesis
NM_006579	EBP	-1.54	-1.58		-1.25	-1.43	emopamil binding protein (sterol isomerase)	Development
NM_001398	ECH1	-1.73	-1.63		-1.27	-1.60	enoyl Coenzyme A hydratase 1, peroxisomal	Cellular lipid metabolism
NM_001404	EEF1G	-1.65	-1.51	-1.29	-1.30	-1.44	eukaryotic translation elongation factor 1 gamma	Protein metabolism
NM_013234	EIF3S12	-1.66	-1.28		-1.27	-1.12	eukaryotic translation initiation factor 3, subunit 12	Unknown
NM_003756	EIF3S8	-1.45	-1.51		-1.55	-1.62	eukaryotic translation initiation factor 3, subunit 3 gamma, 40 kDa	Protein metabolism
BC047866	ENST 00000265423	-1.78	-1.26		-1.12	-1.06	chromosome 6 open reading frame 62, mRNA (cDNA clone MGC:57512 IMAGE:6499979)	Unknown
NM_004446	EPRS	-1.96	-1.91			-1.24	glutamyl-prolyl-tRNA synthetase	Protein metabolism
NM_144503	F11R	-1.10	-1.14		-1.56	-1.36	F11 receptor	Immune response
NM_004470	FKBP2	-2.51	-2.09	-1.09	-1.73	-1.55	FK506 binding protein 2, 13 kDa, transcript variant 1	Protein metabolism
NM_003910	G10	-1.59	-1.78	1.16	-1.48	-1.28	maternal G10 transcript	Transcrition
NM_002047	GARS	-1.70	-1.61	1.02	-1.56	-1.36	glycyl-tRNA synthetase	Protein metabolism
NM_014394	GHITM	-1.79	-1.88		-2.24	-1.70	growth hormone inducible transmembrane protein	Unknown
NM_006098	GNB2L1	-1.02	-1.13	-1.26	-1.55	-1.36	guanine nucleotide binding protein (G protein), beta polypeptide 2-like 1	Cell communication
NM_000183	HADHB	-1.57				-1.61	hydroxyacyl-Coenzyme A dehydrogenase/3-ketoacyl-Coenzyme A thiolase/enoyl-Coenzyme A hydratase (trifunctional protein), beta subunit	Cellular lipid metabolism

Table 1 ***Continued***

Accession No.	Gene symbol	1#	2#	3#	4#	5#	Gene description	Biological process
NM_080820	HARS2		-2.56		-1.60	-1.31	histidyl-tRNA synthetase 2	Amino acid metabolism
NM_178580	HM13	-1.49	-1.14		-1.82	-1.51	histocompatibility (minor) 13	Unknown
NM_001540	HSPA9B	-2.03	-1.82	-1.12	-2.28	-1.57	heat shock 70 kDa protein 9B (mortalin-2), nuclear gene encoding mitochondrial protein	Cell cycle
NM_006764	IFRD2	-1.51	-1.42			-1.20	interferon-related developmental regulator 2	Development
NM_000210	ITGA6	-1.82	-1.42		-1.10	-1.29	integrin, alpha 6	Cell adhesion
NM_002229	JUNB	-1.19	-1.83		-1.79	-2.13	jun B proto-oncogene	Transcrition
NM_015005	KIAA0284	-1.12	-1.26		-1.63	-1.29	KIAA0284	Unknown
NM_000421	KRT10	-1.24	-1.29	-1.05	-1.76	-1.50	keratin 10 (epidermolytic hyperkeratosis; keratosis palmaris et plantaris)	Development
NM_000422	KRT17	1.54	1.25	1.37	1.73	1.85	keratin 17	Development
NM_004138	KRTHA3A	-1.47	-1.67	-1.30	-1.43	-1.02	keratin, hair, acidic, 3A	Unknown
NM_005561	LAMP1	-1.94	-1.83	-1.23	-1.47	-1.41	lysosomal-associated membrane protein 1	Unknown
NM_018407	LAPTM4B	-1.54			-1.42	-1.34	lysosomal-associated protein transmembrane 4 beta	Unknown
M_002300	LDHB	-1.33	-1.49	1.08	-1.44	-1.62	lactate dehydrogenase BN	Glucose metabolism
NM_031484	MARVELD1	-1.89	-2.13		-1.53	-1.49	MARVEL domain containing 1	Unknown
NM_014874	MFN2	-1.53	-1.48		-1.26	-1.22	mitofusin 2, nuclear gene encoding mitochondrial protein	Cell cycle
NM_014046	MRPS18B	-1.90	-1.74				mitochondrial ribosomal protein S18B, nuclear gene encoding mitochondrial protein	Protein metabolism
NM_002467	MYC	-1.48	-2.64			-1.74	v-myc myelocytomatosis viral oncogene homolog (avian)	Cell cycle
NM_004559	NSEP1	-1.38	-1.45	1.24	-1.44	-1.55	nuclease sensitive element binding protein 1	Transcrition
NM_000918	P4HB	-1.65	-1.63		-1.81	-1.27	procollagen-proline, 2-oxoglutarate 4-dioxygenase, beta polypeptide (protein disulfide isomerase-associated 1)	Protein metabolism
NM_005742	PDIA6	-2.35	-2.52		-1.65	-1.46	protein disulfide isomerase family A, member 6	Unknown
NM_024895	PDZK7	-1.53	-1.47	-2.11	-1.53	1.02	PDZ domain containing 7	Unknown
NM_203473	PORCN	-2.87	-2.43	-1.07	-1.49	-1.47	porcupine homolog (Drosophila) (PORCN), transcript variant B	Unknown
NM_138689	PPP1R14B	-1.35	-1.40	1.02	-1.49	-1.68	protein phosphatase 1, regulatory (inhibitor) subunit 14B	Unknown
NM_000310	PPT1	-1.97	-1.97		-1.53	-1.43	palmitoyl-protein thioesterase 1 (ceroid-lipofuscinosis, neuronal 1, infantile)	Protein metabolism
NM_012094	PRDX5	-1.76	-1.58		-1.07	-1.07	peroxiredoxin 5, nuclear gene encoding mitochondrial protein, transcript variant 1	Immune response
NM_212472	PRKAR1A	-1.28	-1.34		-1.52	-1.66	protein kinase, cAMP-dependent, regulatory, type I, alpha (tissue specific extinguisher 1)	Cell communication
NM_002862	PYGB	-2.51	-1.55		-2.67	-1.75	phosphorylase, glycogen; brain	Protein metabolism
NM_000967	RPL3	-1.56	-1.71	-1.02	-1.51	-1.33	ribosomal protein L3	Protein metabolism
NM_000968	RPL4	-1.45	-1.57	-1.32	-1.36	-1.16	ribosomal protein L4	Protein metabolism
NM_033251	RPL13	-1.25	-1.34		-1.30	-1.74	ribosomal protein L13	Protein metabolism
NM_002948	RPL15	-1.35	-1.57	1.19	-1.53	-1.52	ribosomal protein L15	Protein metabolism
NM_033251	RPL30	1.37	1.35	1.06	1.68	1.42	ribosomal protein L30	Protein metabolism
NM_033625	RPL34	1.47	1.32	-1.30	1.75	1.51	ribosomal protein L34	Protein metabolism
NM_053275	RPLP0	-1.29	-1.49	1.10	-1.17	-1.55	ribosomal protein, large, P0	Protein metabolism

Table 1 ***Continued***

Accession No.	Gene symbol	1#	2#	3#	4#	5#	Gene description	Biological process
NM_002950	RPN1	-2.03	-1.65			-1.59	*Homo sapiens* ribophorin I	Protein metabolism
NM_001005	RPS3	-1.57	-1.66	-1.34	-1.18	-1.02	ribosomal protein S3	Protein metabolism
NM_183352	SEC13L1	-1.51	-1.26		-1.02	-1.20	SEC13-like 1 (*S. cerevisiae*), transcript variant 2	Development
NM_006640	SEPT9	-1.27	-1.78		-1.29	-1.53	septin 9	Unknown
NM_152264	SLC39A14	-1.62	-1.55		-1.29	-1.21	solute carrier family 39 (zinc transporter), member 13	Unknown
NM_014426	SNX5	-1.16	-1.26		-1.53	-1.35	Sorting Nexin 5	Cell communication
NM_021102	SPINT2	-1.57	-1.67	1.07	-1.14	-1.23	serine protease inhibitor, Kunitz type, 2	Cell motility
NM_003145	SSR2	-1.22	-1.36	-1.14	-1.58	-1.38	signal sequence receptor, beta (translocon-associated protein beta)	Cell organization and biogenesis
NM_003146	SSRP1	-1.20			-1.69	-1.22	structure specific recognition protein 1	Transcrition
NM_152295	TARS	-1.24	-1.57		-2.05	-1.19	threonyl-tRNA synthetase	Protein metabolism
NM_012458	TIMM13	-1.63	-1.45	-1.02	-1.07	-1.35	translocase of inner mitochondrial membrane 13 homolog (yeast), nuclear gene encoding mitochondrial protein	Development
NM_003722	TP73L	-1.51	-2.42	1.08	-1.82	-1.40	tumor protein p73-like	Cell communication
NM_003329	TXN	1.69	2.06		2.21	1.98	thioredoxin	Cell communication
NM_005080	XBP1	-1.61	-1.68		-1.64	-1.41	X-box binding protein 1	Transcrition
NM_003404	YWHAB	-1.58	-1.46	1.49	-1.45	-1.61	tyrosine 3-monooxygenase/tryptophan 5-monooxygenase activation protein, beta polypeptide, transcript variant 1	Unknown
CLUSTER III								
NM_006317	BASP1	1.85	1.88		1.88	1.42	brain abundant, membrane attached signal protein 1	Unknown
NM_000610	CD44	1.83	1.78	1.52	1.92	1.31	CD44 antigen	Cell adhesion
NM_133467	CITED4	2.19	2.32		2.02	1.67	Cbp/p300-interacting transactivator, with Glu/Asp-rich carboxy-terminal domain, 4	Transcrition
NM_024045	DDX50	1.71	1.63			1.47	DEAD (Asp-Glu-Ala-Asp) box polypeptide 50	Unknown
NM_001967	EIF4A2	2.28	1.98		1.41	1.63	eukaryotic translation initiation factor 4A, isoform 2	Protein metabolism
NM_004004	GJB2	2.49	1.95		1.47	2.21	gap junction protein, beta 2, 26 kDa (connexin 26)	Cell communication
NM_004832	GSTO1	2.52	4.80			2.73	glutathione S-transferase omega 1	Unknown
NM_005345	HSPA1A	2.06	2.14		1.38	1.46	heat shock 70 kDa protein 1A	Cell cycle
NM_006644	HSPH1	1.55	1.61			1.21	heat shock 105 kDa/110 kDa protein 1	Protein metabolism
NM_002658	PLAU	2.22	2.85		2.30	1.87	plasminogen activator, urokinase	Cell communication
NM_002835	PTPN12	2.05	2.43			1.24	protein tyrosine phosphatase, non-receptor type 12	Protein metabolism
NM_002872	RAC2	2.89	3.88		2.10		ras-related C3 botulinum toxin substrate 2	Cell communication
NM_000539	RHO	1.74	1.69				rhodopsin (opsin 2, rod pigment)	Cell communication
NM_020150	SARA1	1.75	1.84			2.04	SAR1a gene homolog 1 (*S. cerevisiae*)	Cell communication
NM_021199	SQRDL	1.90	1.92		1.59	1.38	sulfide quinone reductase-like (yeast)	Unknown
NM_020182	TMEPAI	1.73	2.34	1.59	2.48	1.80	transmembrane, prostate androgen induced RNA, transcript variant 1	Cell communication
NM_005499	UBA2	1.67	1.48		1.10	1.21	SUMO-1 activating enzyme subunit 2	Protein metabolism
CLUSTER IV								
NM_005946	MT1A	1.64	1.52	1.85	4.11	2.26	metallothionein 1A (functional)	Unknown
NM_005947	MT1B	1.72	1.84	2.37	5.00	2.70	metallothionein 1B (functional)	Unknown
NM_175617	MT1E	1.49	1.63	2.33	4.40	2.81	metallothionein 1E (functional)	Unknown
NM_005950	MT1G	1.92	1.88	2.25	5.23	2.71	metallothionein 1G	Unknown
NM_005951	MT1H	1.87	1.84	2.28	4.68	2.68	metallothionein 1H	Unknown

Table 1 ***Continued***

Accession No.	Gene symbol	1#	2#	3#	4#	5#	Gene description	Biological process
NM_005952	MT1X	1.88	1.76	2.28	4.54	2.48	metallothionein 1X	Development
NM_005953	MT2A	2.21	2.09	2.57	6.38	2.86	metallothionein 2A	Metal ion homeostasis
BC007034	ENST 00000245185	2.26	2.14	2.35	5.95	3.20	metallothionein 2A, mRNA (cDNA clone MGC:12397 IMAGE:4051220)	Metal ion homeostasis
CLUSTER V								
NM_001101	ACTB	1.19	1.14	1.21	1.51	1.29	actin, beta	Cell cycle
NM_001102	ACTN1				2.08	2.23	actinin, alpha 1	Unknown
NM_004039	ANXA2	1.26	1.32	1.20	1.55	1.29	Annexin A2	Development
NM_006476	ATP5L	1.41	1.23		1.83	1.64	ATP synthase, H^+ transporting, mitochondrial F0 complex, subunit g, nuclear gene encoding mitochondrial protein	Phophorylation
NM_178508	C6orf1	1.39	1.34		1.98	1.67	chromosome 6 open reading frame 1	Unknown
NM_016289	CAB39				2.01	1.77	calcium binding protein 39	Unknown
NM_006367	CAP1	1.47	1.44		1.84	1.30	adenylate cyclase-associated protein 1 (yeast)	Unknown
NM_152221	CSNK1E	1.60	1.22	1.16	1.60	1.33	casein kinase 1, epsilon, transcript variant 1	Cell communication
AK074742	ENST 00000361624	-2.28	-1.38	-2.38	-1.49	-2.09	cDNA FLJ90261 fis, clone NT2RM4000761	Unknown
NM_001997	FAU	1.15	1.10	1.03	1.53	1.60	Finkel-Biskis-Reilly murine sarcoma virus (FBR-MuSV) ubiquitously expressed (fox derived); ribosomal protein S30 (FAU)	Protein metabolism
NM_001436	FBL	-1.24	-1.57		-1.03	-1.14	fibrillarin	RNA metabolism
M90686	HLA-G				2.95	3.24	lymphocyte antigen (HLA-G3)	Immune response
NM_001540	HSBP1		1.86		1.87	1.92	heat shock 27 kDa protein 1	Transcrition
NM_000576	IL1B	1.25	1.41		2.26	1.39	interleukin 1, beta	Immune response
NM_002192	INHBA	1.40	1.55		3.20	1.77	inhibin, beta A (activin A, activin AB alpha polypeptide)	Cell cycle
NM_002305	LGALS1	1.55	1.18	1.22	2.25	1.36	lectin, galactoside-binding, soluble, 1 (galectin 1)	Cell communication
NM_004528	MGST3				2.23	1.59	microsomal glutathione S-transferase 3	Immune response
NM_079423	MYL6	1.49	1.40	-1.24	2.12	1.67	myosin, light polypeptide 6, alkali, smooth muscle and non-muscle	Development
NM_004552	NDUFS5	1.19	1.25	-1.07	1.58	1.63	NADH dehydrogenase (ubiquinone) Fe-S protein 5, 15 kDa (NADH-coenzyme Q reductase) (NDUFS5)	Phophorylation
NM_002624	PFDN5	1.55	1.09		1.68	1.37	prefoldin 5, transcript variant 1	Protein metabolism
NM_007273	PHB2	-1.66	-1.50	1.11	-1.68	-1.76	prohibitin 2	Unknown
NM_021128	POLR2L	1.34	1.33		1.91	1.45	polymerase (RNA) II (DNA directed) polypeptide L, 7.6 kDa	Transcrition
NM_002791	PSMA6	1.41	1.18		1.91	1.92	proteasome (prosome, macropain) subunit, alpha type, 6	Protein metabolism
NM_006263	PSME1	1.04	1.29		2.09	1.85	proteasome (prosome, macropain) activator subunit 1 (PA28 alpha)	Immune response
NM_006907	PYCR1	-2.57	-1.89	-1.00	-1.47	-1.36	pyrroline-5-carboxylate reductase 1, transcript variant 1	Development
NM_175744	RHOC	1.30	1.28		1.57	1.28	ras homolog gene family, member C	Unknown
NM_001026	RPS24	1.33	1.31	-1.19	1.71	1.68	ribosomal protein S24	Protein metabolism
NM_005979	S100A13	1.62	1.63		1.64	1.38	S100 calcium binding protein A13, transcript variant 2	Development
NM_005978	S100A2	1.26	1.24	-1.27	2.29	1.59	S100 calcium binding protein A2	Development
NM_001018108	SERF2	1.27	1.49	1.09	1.71	1.78	small EDRK-rich factor 2	Unknown
NM_004607	TBCA	1.53	1.32		1.63	1.50	tubulin-specific chaperone a	Protein metabolism

Table 1 ***Continued***

Accession No.	Gene symbol	1#	2#	3#	4#	5#	Gene description	Biological process
NM_207013	TCEB2	1.22	1.26		1.85	1.89	transcription elongation factor B (SIII), polypeptide 2 (18 kDa, elongin B)	Protein metabolism
THC2276562	THC2276562	1.24	1.69	-1.31	1.96	2.56	limbic system-associated membrane protein	Unknown
NM_021103	TMSB10	1.40	1.27	1.09	1.76	1.38	thymosin, beta 10	Cell organization and biogenesis
NM_000365	TPT1	1.64	1.26	-1.34	1.73	1.43	triosephosphate isomerase 1	Cell cycle
NM_006086	TUBB3	1.66	1.56		1.71	1.52	tubulin, beta 3	Unknown
NM_006701	TXNL4A	-1.21	-1.18		-1.59	-1.23	thioredoxin-like 4A	Unknown
NM_024292	UBL5	1.46	1.57		2.21	1.87	ubiquitin-like 5	Protein metabolism
NM_003761	VAMP8	1.19	1.23		1.66	1.72	vesicle-associated membrane protein 8	Protein metabolism
NM_006373	VAT1	1.86	1.69		2.23	1.58	vesicle amine transport protein 1 homolog (T californica)	Development
NM_006887	ZFP36L2				2.37	2.54	zinc finger protein 36, C3H type-like 2	Cell proliferation

*A total of 162 genes were identified from the five SMG experiments to be significantly ($\geq$1.5-fold change, $p \leq 0.05$) differentially expressed. They were further categorized into 5 clusters and 18 functional groups. #1. Regulation value of 3-day SMG. #2. Regulation value of 4-day SMG. #3. Regulation value of 4-day SMG plus 15-day recovery. #4. Regulation value of 9-day SMG plus 50-day recovery. #5. Regulation value of 10-day SMG plus 60-day recovery.